

Origin of the gossamer ferromagnetism in MnTe

I. I. Mazin

*Department of Physics and Astronomy, George Mason University, Fairfax, VA 22030, USA and
Quantum Science and Engineering Center, George Mason University, Fairfax, VA 22030, USA*

Absence of net magnetization in altermagnetism is both a blessing (no stray fields) and a curse (no obvious way to manipulate altermagnetic domains by external fields). Yet, MnTe was demonstrated experimentally to have no measurable stray fields and yet controllable by external magnetic field — a win-win situation. In this paper we discuss possible mechanisms driving this ultra-small canting of Mn moments, and, most importantly, the microscopic mechanism of coupling the canting with the altermagnetic order. It appears to be a higher (third) order effect in (already very small) spin-orbit coupling, which explains the unusually weak, barely measurable ferromagnetism in MnTe. Microscopic understanding of the beneficial properties of MnTe opens a road to controllable design of similar altermagnets for spintronics applications.

I. INTRODUCTION

Altermagnetism has attracted a lot of attention recently[1–3]. Both novel physical phenomena and potential applications with orders of magnitude better performance have been discussed. Already more than a hundred of altermagnets have been identified among existing antiferromagnets or predicted theoretically.

Nevertheless, nearly all experimental studies so far have been performed on a handful of materials. Till recently, the most popular was RuO₂, where in 2017 weak antiferromagnetism (Ru moments $\sim 0.05 \mu_B$) was reported in neutron scattering experiment[4], with an altermagnetic ordering pattern. Close to 25 papers have been published in the last few years claiming various altermagnetic manifestations. Unfortunately, in most cases an interpretation in terms of altermagnetism required and order-of-magnitude moment than that reported in Ref. [4], and, to add insult to injury, it was recently shown that even the reported moment was an artifact resulting from multiple neutron scattering and in reality RuO₂ is nonmagnetic both in bulk and in films[5, 6], albeit may be magnetic in a few atomic layer form[7].

The second in popularity altermagnetic candidate is Mn₅Si₃. There the problem is different. The material is well studied experimentally, and three ordered magnetic phases exist in the bulk[8–10], one collinear and two noncollinear. However, all three order with the vector $\{0,1/2,0\}$, so by definition not altermagnetic. An argument was put forward that in thin films the order can switch spontaneously to $\{0,0,0\}$, but the fact that three different magnetic patterns share the same ordering vector suggests existence of strong antiferromagnetic coupling between the neighboring along the b direction unit cells, which would be difficult to overcome in thin films.

This leaves with the third by popularity compound, MnTe. This is truly a poster child for the altermagnetic case. Its magnetic structure is perfectly well known, and is definitely antiferromagnetic. It is self-doped (hole concentration $\sim 10^{18} \text{ cm}^{-3}$ [11]), and the Néel vector is in the 210 direction, which is the one compatible with the

anomalous transport. As I will discuss in this paper, it also possesses a fortuitous combination of other parameters, making it truly an ideal candidate for both studying the altermagnetic physics and for spintronics applications.

II. MNTE: BACKGROUND

MnTe, despite being a canonical Mott (or, more correctly, charge transfer) insulator has been known to occur always in a self-doped form, exhibiting a sizeable conductivity and also showing anomalous Hall conductivity (AHC), discovered as early as in 1965[12]. The fact that AHC is present in an antiferromagnetic material was either ignored[13] or ascribed to weak ferromagnetism of unknown origin[12]. Recently, the interest in anomalous transport in MnTe was rekindled after researchers realized that it is altermagnetic[1–3, 14]. AHC has been remeasured[15–18], and weak ferromagnetism detected and its amplitude estimated to be $\sim 2.5 \times 10^{-5}$ [18] to 5×10^{-5} [16] μ_B/Mn , parallel to c . Furthermore, it has been now realized that the magnetization is too small to explain the large observed AHC, which then must have the altermagnetic origin.

Regarding the origin of this extremely weak (“gossamer”) ferromagnetism, different hypotheses were offered. In the earliest paper[12] it was pointed out that the magnetic space group (MSG) Cm' c 'm, which is realized in MnTe[19], is, per Turov's classification[20], compatible with ferromagnetism, while no assumptions were made about the microscopic nature of the latter. In several later papers[17, 21] it was suggested that excess of Mn may lead to weak ferromagnetism. Similarly, in Ref. [16] an empirical energy expression, compatible with the MSG, was introduced, with a remark (quite correct) that the standard Dzyaloshinskii-Moriya interaction (DMI) cannot generate this expression.

However, a possibility of excess (interstitial) Mn or Te vacancies seems unlikely given that in such a case one would expect electron, not hole doping. So the question of microscopic origin of the weak ferromagnetism remains

TABLE I. Three weak effects combining to provide altermagnetic domain control by an external field. Here H is the field, x is the hole concentration, t characterizes one-electron hopping amplitude near the Fermi level, J is a gauge of the average Heisenberg coupling, and M is the Mn magnetic moment, $\approx 5 \mu_B$. The last two line, emphasized in italics, introduce two other effects, not present in MnTe, which may however appear in other altermagnetic materials. Note that double exchange canting does not couple to altermagnetism on its own, but can couple when assisted by DMI-type interactions.

effect	provides	order of magnitude
Feedback of spin polarization on charge distribution	symmetry lowering	SOC ²
DMI in the symmetry-lowered structure	coupling between ferromagnetism and altermagnetism	SOC
External field	Zeeman coupling with weak ferromagnetism	H
<i>Double exchange</i>	<i>Weak ferromagnetism</i>	<i>Mtx/J</i>
<i>Single site anisotropy</i>	<i>Weak ferromagnetism and coupling to altermagnetism</i>	SOC ²

open.

In this paper, we will demonstrate that concerted action of three separate mechanisms leads to a small magnetic canting and controlled altermagnetism. In a nutshell, there is one effect, quadratic in spin-orbit coupling, the feedback of altermagnetic ordering on the charge distribution, which marginally lowers the (charge) space group from # 194 (P6₃/mmc) to #63 (Cmcm). The other effect is a DMI interaction that couples the already existing weak ferromagnetic component with altermagnetism, thus allowing to manipulate altermagnetic domains with a external magnetic field. This effect only appears because of the symmetry lowering described above, and is therefor proportional to the third power of weak spin-orbit coupling. And, of course, the third effect is rather trivial: Zeeman coupling of the external field with the ferromagnetic component. This is summarized in Table I.

III. ANISOTROPIC EXCHANGE COUPLING IN MNTE

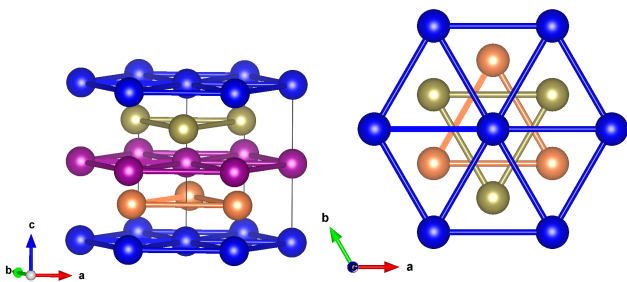


FIG. 1. Blue: Mn up; purple: Mn down; orange, olive: Te

In this Section, I will construct the full 3×3 exchange matrices for the first three Mn-Mn bonds, and will show that they cannot induce a uniform canting. A full exchange matrix for a bond $I = 1, 2, 3$ is defined such that

its energy is

$$E^{(I)} = \sum_{\alpha\beta} \mathbf{m}_1 \cdot \mathcal{J} \cdot \mathbf{m}_2', \quad (1)$$

where \mathbf{m} s are unit vectors in the direction of the Mn moments at the ends of the bond, and

$$\mathcal{J} = \begin{pmatrix} J_{xx} & J_{xy} & J_{xz} \\ J_{yx} & J_{yy} & J_{yz} \\ J_{zx} & J_{zy} & J_{zz} \end{pmatrix} \quad (2)$$

For a reference, I quote the calculated values of the isotropic (Heisenberg) exchange ($J = (J_{xx} + J_{yy} + J_{zz})/3$ in these three cases. The nearest neighbor bond, which is perpendicular to the basal plane, is strongly antiferromagnetic (AF), $J_1 = 42.1$ meV, the next nearest neighbor bond (the nearest inside the plane) has $J_2 \approx 0$, and the third, which is just the sum of the other two, is also AF, $J_3 = 5.3$ meV.

To begin with, let us show that there is no DMI interaction on the nn (AF) bond. Indeed, there is a 001 mirror plane through the midpoint, which indicates that the DMI vector $\mathbf{D} \perp \hat{\mathbf{z}}$. There are also three mirrors passing through the bond itself, namely 100, 010 and 110. \mathbf{D} must be perpendicular to each of them, which is impossible. Moreover, a detailed analysis shows that the full exchange matrix for this bonds is exceedingly simple:

$$\mathcal{J} = \begin{pmatrix} J & 0 & 0 \\ 0 & J & 0 \\ 0 & 0 & J + J_z \end{pmatrix} \quad (3)$$

i.e., only the J_z Ising exchange is allowed besides the Heisenberg exchange.

The nn in the planes are not DMI because of inversion. Second nn across the plane (depicted in Fig. 2) have a C_2 passing through the midpoint, namely for the $10\frac{1}{2}$ bond the axis is 010. \mathbf{D} is then perpendicular to this axis, that is, lies in the xz plane. Let us consider this interaction more closely. There are 12 bonds of this kind, which I will label as i, s , where $i = 1..6$ are rotations around 001

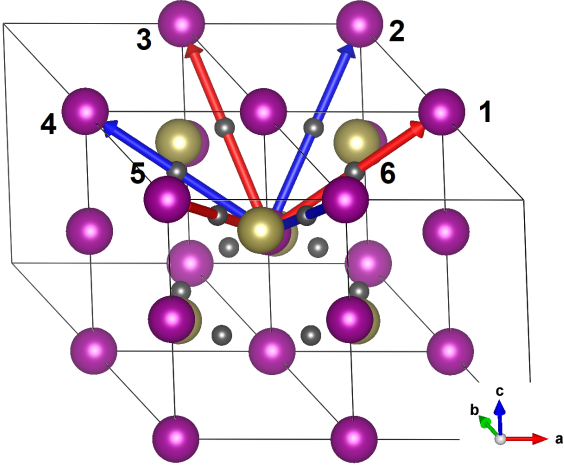


FIG. 2. Labeling of the Mn atoms (the upper 6) and DMI bonds (bond centers depicted with grey balls). The same color bonds (and their inversion partners) are equivalent in the local coordinate system explained in the text. For instance, for the bond 1 the local system coincides with the global one, x, y, z , and for the others it is rotated in steps of $\pi/3$

and $s = \pm$ indicates where the bond is going up or down. Let me also write the full exchange matrix as

$$\hat{j}^{is} = \begin{pmatrix} J_{XX}^{is} & J_{XY}^{is} & J_{Xz}^{is} \\ J_{YX}^{is} & J_{YY}^{is} & J_{Yz}^{is} \\ J_{zX}^{is} & J_{zY}^{is} & J_{zz}^{is} \end{pmatrix} \quad (4)$$

where the new axis X is the projection of the bond onto the ab plane, and Y is perpendicular to X, z . Note that it is enough to consider only $s = +$, because due to the inversion $\hat{j}^{1-} = \hat{j}^{4+}$, $\hat{j}^{2-} = \hat{j}^{5+}$, $\hat{j}^{3-} = \hat{j}^{6+}$, etc. As mentioned, there is only one operation that keeps a bond in place, C_{2Y} , which transforms $S_X \rightarrow -S_X$, $S_Y \rightarrow S_Y$, $S_Z \rightarrow -S_Z$, so

$$\begin{pmatrix} J_{XX} & J_{XY} & J_{Xz} \\ J_{YX} & J_{YY} & J_{Yz} \\ J_{zX} & J_{zY} & J_{zz} \end{pmatrix} = \begin{pmatrix} J_{XX} & -J_{YX} & J_{zX} \\ -J_{XY} & J_{YY} & -J_{zY} \\ J_{Xz} & -J_{Yz} & J_{zz} \end{pmatrix} \quad (5)$$

$$= \begin{pmatrix} J_{XX} & D_z & A \\ -D_z & J_{YY} & D_X \\ A & -D_X & J_{zz} \end{pmatrix}, \quad (6)$$

therefore $J_{Xz} = J_{zX} = A$, $J_{XY} = -J_{YX} = D_z$, $J_{zY} = -J_{zX} = D_X$.

Next, consider a mirror plane through the origin and the Te atoms. One such plane converts J^1 to J^2 , and it also changes $S_X \rightarrow -S_X$, $S_Y \rightarrow S_Y$, $S_Z \rightarrow -S_Z$. Then

$$\begin{pmatrix} J_{XX}^1 & D_z^1 & A^1 \\ -D_z^1 & J_{YY}^1 & D_X^1 \\ A^1 & -D_X^1 & J_{zz}^1 \end{pmatrix} = \begin{pmatrix} J_{XX}^2 & -D_z^2 & A^2 \\ D_z^2 & J_{YY}^2 & -D_X^2 \\ A^2 & D_X^2 & J_{zz}^2 \end{pmatrix}, \quad (7)$$

That is, the compass term A is the same, the z -component of the DMI vector changes sign, and also the

radial vector. The result is shown in Fig. 3, where the red arrows give the local X axis (the radial component of the DMI vector, blue, is parallel). Since the alternating Néel vector lies in the plane, the compass terms has no effect, and the DMI field exerted by the parallel to each other spin-up moments onto the the spin down subsystem cancel out. Note that this cancellation is a direct consequence of the 3-fold rotational axis.

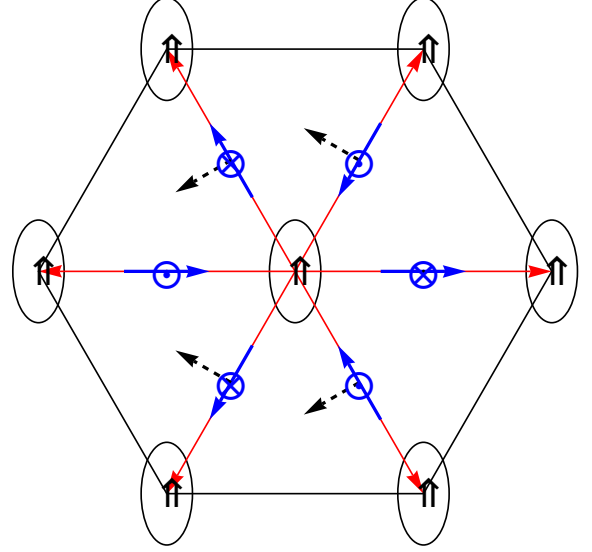


FIG. 3. DMI interaction. Dotted and crossed circles show $\pm D_z$, the blue arrows D_X , and the dashed black ones the small (tiny!) components that arise from the feedback of the magnetic symmetry breaking.

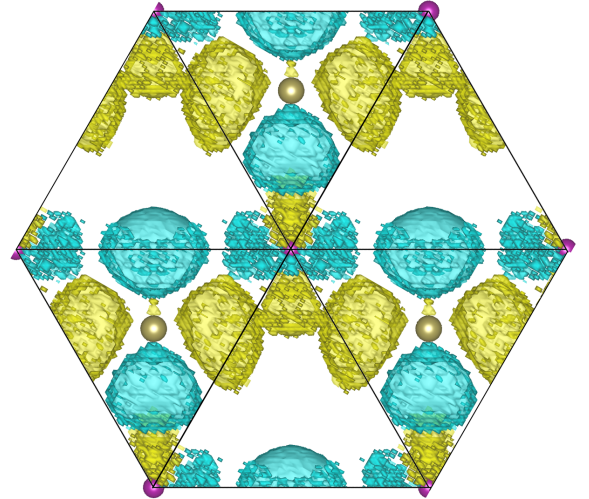


FIG. 4. Difference between the charge densities of the 210 Néel vector (the ground state) and the 100 one. The colors indicate the sign, and isosurfaces are drawn at the level of $2 \times 10^{-6} e/\text{\AA}^3$ (about 4 orders of magnitude less than the total charge density). Note breaking of the C_3 rotational symmetry.

However, that does not account for the magnetic order already affecting the crystal symmetry. As long as there is spin-orbit coupling, there will be an additional very small change in the charge distribution ($\propto M^2$) that breaks the hexagonal symmetry of the charge cloud, as shown (exaggerated) in Fig. 4.

In Fig. 4 I show results of DFT calculation using the VASP code[22, 23]. Charge density was calculated self-consistently, including SOC, for the Néel vector $\mathbf{M}||210$ and the perpendicular to it vector $\mathbf{M}||100$. A very fine k -point mesh of $21 \times 21 \times 11$ was used, with the convergence criterion of 10^{-8} eV and an energy cut-off of 800 eV. In order to avoid systematic error, both calculations were started with a self-consistent calculation with $\mathbf{M}||001$, and then the spin coordinate system was rotated using the SAXIS tag in VASP. The same protocol applied to nonrelativistic calculations did not produce any symmetry breaking.

Because of this symmetry breaking, the mirror σ_Y remains only for the bonds J^1 and J^4 , but is broken for the others (and, of course, C_3 is broken as well). As a result, the in-plane vector D_x is not strictly radial any more for the other bonds, but acquires a tiny tangential component D_y .

Let me now concentrate on the bonds J^2 and J^3 . There still is a mirror relating the two bonds. However, there is no condition any more that $D_Y = 0$. Keeping only the DMI terms,

$$\begin{pmatrix} D_z^3 & D_Y^3 \\ -D_z^3 & D_X^3 \\ -D_Y^3 & -D_X^3 \end{pmatrix} = \begin{pmatrix} -D_z^2 & D_Y^2 \\ D_z^2 & -D_X^2 \\ -D_Y^2 & D_X^2 \end{pmatrix}, \quad (8)$$

That is to say, there appears a small tangential component D_Y .

Now we need to connect that to $J^{5,6}$. There is a C_{2x} axis. It will convert J^2 to J^6 , and, in the original Cartesian system, $S_x \rightarrow S_x$, $S_y \rightarrow -S_y$, $S_z \rightarrow -S_z$. Without going into details, it means that the J_{yz} component will not change, that is, D_x will remain the same, and will have a net component after averaging, as shown in Fig. 3 by the dashed arrows. Per Table 1, this interaction scaled as cube of SOC.

While we do not make any attempt to cast this interaction into a gauge-invariant form, from general symmetry considerations one can conclude that this interaction can be written generically as $H = \sum_{ij} (\mathbf{S}_i \cdot \hat{K} \cdot \mathbf{S}_i)(\mathbf{S}_i \times \mathbf{S}_j) \cdot \mathbf{C}_{ij}$, where the tensor \hat{K} is similar to the single-site anisotropy tensor, and \mathbf{C}_{ij} similar to the Dzyaloshinskii-Moriya exchange. It can be compared to the interaction defined by Blügel et al[24] and by Brinker et al[25] (see also Ref. [26]) as “chiral biquadratic interaction”, $H = \sum_{ij} (\mathbf{S}_i \cdot \mathbf{S}_j)(\mathbf{S}_i \times \mathbf{S}_j) \cdot \mathbf{C}_{ij}$.

IV. OTHER POTENTIAL SOURCES OF CANTING

Besides DMI, two other sources for weak ferromagnetism are often discussed in the literature. One is the single site anisotropy, and is known[27] to be the source of canting in NiF_2 . This requires easy axes that are different in the two sublattices. For instance, in the two sublattices in NiF_2 these are $[110]$ and $[\bar{1}\bar{1}0]$. This mechanism also couples with the antiferromagnetic order (note that NiF_2 is an altermagnet), but can manifest itself indirectly as discussed above. In MnTe , however, this mechanism is absent by symmetry: the two magnetic sublattices have exactly the same local symmetry and the same easy axes, namely $[210]$, $[\bar{1}20]$, and $[\bar{1}\bar{1}0]$.

Another mechanism commonly believed to be a possible source for weak ferromagnetism is double exchange, proposed by Zener in 1951[28], and by now a part of all standard textbooks on magnetism [29]. In the essence, it is a competition between antiferromagnetic exchange among (reasonably well) localized moments, which wants to keep the latter antiparallel, and the kinetic energy of the itinerant electrons, assuming that there is a strong interaction keeping itinerant electrons' spins locally parallel to the localized moments. This interaction can be Hund's rule coupling (combined with the Hubbard U), or, if the itinerant electrons originate from different atomic species, Schrieffer-Wolff interaction[30] (which would have been the case in the charge-transfer insulator MnTe). Conventionally, the corresponding Hamiltonian is written under the assumptions that (a) the undoped material is insulating, (b) the Hund's rule coupling is infinite, so electron hopping along an antiferromagnetic bond is fully arrested and (c) all nearest neighbor bonds are antiferromagnetic and hopping to all other neighbors is neglected. The model is usually illustrated on a 1D Néel antiferromagnet. In that case, in a fully collinear antiferromagnetic state the doping proceeds through a zero-width band and the kinetic energy of the doped carriers can be lowered by canting the local spins and allowing for some hopping, which in this case scales as the sine of the canting angle ϕ , and the Hamiltonian reads[29]:

$$E = -aJ \cos 2\phi - bxt \sin \phi, \quad (9)$$

where E is the total energy per spin, J is a properly averaged antiferromagnetic exchange coupling, x is the concentration of itinerant carriers (assumed $x \ll 1$), t is the hopping parameter of the itinerant electrons, and a and b are geometrical coefficients characterizing the connectivity in the system. ϕ is the canting angle away from the original collinear antiferromagnetic arrangement. Minimizing this expression, one gets

$$\sin \phi = (bt/4aJ)x, \quad (10)$$

that is to say, the net ferromagnetic moment is linearly proportional to the concentration x .

As often happens in an idealized scenario, the assumptions above — which can be quantified as $t^2/J_H \ll t \sin \phi$

and $t' \ll t \sin \phi$, where t' characterizes the same-spin hopping to farther neighbors — come into question in the real life. In particular, it is clear that no matter what are the materials parameters, the conditions will be violated at sufficiently small ϕ . Moreover, the time-reversal symmetry implies that at $\phi \rightarrow 0$ a linear in canting term cannot be allowed.

Generally speaking, if there are several different channels for one-electron hopping, they add in quadrature, so the effective hopping amplitude $t \sin \phi$ in Eq. 9 should be replaced with $\sqrt{(t \sin \phi)^2 + (ut^2/J_H)^2 + (vt')^2}$, where u and v are coefficients of the order 1. The last two terms can be estimated from the band structure calculation, since they determine the bands width in the antiferromagnetic case.

Let us assess to what extent these criteria are fulfilled in MnTe. To this end, we can compare bands in the collinear A-type antiferromagnetic case with those in the ferromagnetic one. Since the in-plane order is collinear in both cases, the problem maps exactly onto a 1D antiferromagnetic chain, which makes this comparison particularly straightforward. Fig. 5 shows that the effective z -hopping $\sqrt{(ut^2/J_H)^2 + (vt')^2}$ is nearly 200 meV, albeit becomes nearly twice smaller than the ferromagnetic hopping, $\sqrt{(t \sin \phi)^2 + (ut^2/J_H)^2 + (vt')^2} \approx 340$ meV, and $t \sin \phi \approx 280$ meV. Obviously, despite seeming favorable case (1D hopping, large onsite spin-flip energy cost), the double exchange model is not applicable to MnTe.

To verify this conclusion, we have calculated the total energy as a function of the weak ferromagnetic moment, using the VASP constrained-directions mode for a sizeable doping of 0.2 hole/Mn (Fig. 6). The calculations show no minimum at any finite canting, and a perfectly quadratic dependence for canting angles up to $\approx 3.5^\circ$ (with a slight bending down at higher angle, reflecting indeed the double exchange physics).

Suppose that an altermagnetic material is allowed to have weak ferromagnetism, but microscopically the mechanism of spin canting does not couple to altermagnetic domains, that is, canting can be flipped without incurring a change in energy even if the altermagnetic order is not flipped. This is for instance in case in easy-plane rutiles. On the first glance such canting is completely useless from the point of view of manipulating altermagnetic domains with an external field. However, if another canting mechanism is present, such as the one described in the previous section, which maybe order(s) of magnitude smaller in amplitude, than the two canting mechanisms couple to each other, and thus the former (stronger) also couples with the altermagnetic order. This is an exciting opportunity that, in principle, allows to manipulate the domains with very small fields, even if the relevant DMI interaction is of a higher order and extremely small. As discussed below, in MnTe this possibility is not realized, but it may prove instrumental in other altermagnetic materials.

As a general note: if altermagnetic material appears to have weak ferromagnetism, but microscopically the

mechanism of spin canting does not couple to altermagnetic domains (as in double exchange mechanism), that is, canting can be flipped without incurring a change in energy even if the altermagnetic order is not flipped, this does not mean that such canting is completely useless from the point of view of manipulating altermagnetic domains with an external field. Indeed, if another canting mechanism is present, such as the one described in the previous section, which maybe order(s) of magnitude smaller in amplitude, than the two canting mechanisms couple to each other, and thus the former (stronger) also couples with the altermagnetic order. This is an exciting opportunity that, in principle, allows to manipulate the domains with very small fields, even if the relevant DMI interaction is of a higher order and extremely small. As discussed below, in MnTe this possibility is not realized, but it may prove instrumental in other altermagnetic materials.

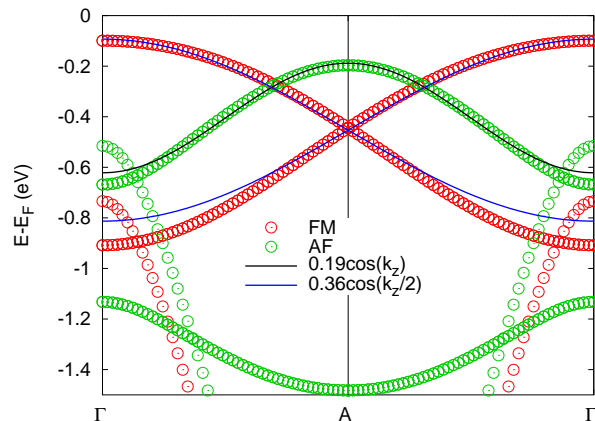


FIG. 5. Band dispersions for the spin-minority channel in ferromagnetic (FM) and altermagnetic (antiferromagnetic, AF) states. The band dispersions near the top of the valence band along the Γ -A direction were fitted to $\cos(ck_z/2)$ and $\cos(ck_z)$, respectively. One can see that while the prefactor in the latter case is nearly twice larger, the effective net hopping along z is nearly 200 meV already in the antiferromagnetic case.

To conclude this section, while in principle there exist other mechanisms for canting not related to DMI interactions and not coupled directly to the altermagnetic order, none of them is operative in MnTe and the observed magnetization is entirely due to the chiral biquadratic interaction described in the previous section.

V. DISCUSSION AND CONCLUSIONS

A major obstacle on the road to exciting spintronics applications is inability to manipulate altermagnetic domains by external stimuli. Indeed, the major advantage of altermagnets over ferromagnets is absence of net magnetization and thus of stray fields. Yet the same zero net magnetization prevents an altermagnet from interacting with external magnetic fields and thus presents

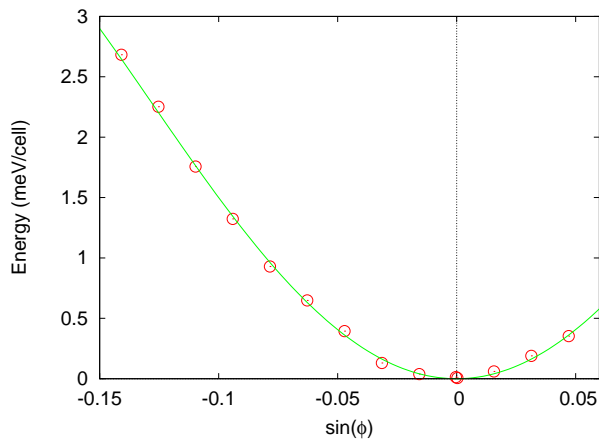


FIG. 6. Energy in the canted state as a function of the canting angle ϕ , assuming hole doping of 0.2 hole/Mn. The line is a fitting to the even-only power polynomial up to the 6th power.

a problem with controlling and manipulating altermagnetic domains. In many cases, in fact in those same cases where anomalous transport in an altermagnet is nonzero, the magnetic point group is compatible with ferromagnetism, a phenomenon known as weak ferromagnetism. However, several prerequisites are necessary before one can take an advantage of this weak ferromagnetic component, namely, the canting of altermagnetic moments need not only be allowed by symmetry, but microscopic interactions must be present generating such canting. Second, this canting must be small enough not to generate stray fields by itself. Third, it has to couple with the altermagnetic order so that flipping the ferromagnetic component would lead to flipping the altermagnetic order.

Three mechanisms are known to generate weak ferromagnetism. One is a single-site anisotropy, as in NiF_2 [27], another double exchange. Neither couples with the altermagnetic order, nor are they present in MnTe. One possibility is Dzyaloshinskii-Moriya interaction, but, as the discussion above exemplifies, absence of an inversion center at the midpoint of a magnetic bond does not guarantee (contrary to a common misconception) presence of such interaction, and even if it is non-zero in most cases it cancels out when summed over all equivalent bonds. Besides, if it is allowed, it is the first order in spin-orbit coupling so may actually be strong enough to generate too large stray fields.

As discussed in this paper, MnTe represents a new

paradigm, applicable to altermagnetic semiconductors (actually the largest subclass of the latter), doped naturally or in a controlled way by a very small number of carriers, 10^{-4} – 10^{-5} per magnetic ion. This doping ensures metallic conductivity required for applications, and, in principle, albeit not in MnTe, may actually enhance the magnetization, if needed for application, via double exchange. Thus, we have three decoupled, that is, controlled by different factors, parameters: altermagnetic transport, which is completely oblivious to the small ferromagnetic component, the four-spin Dzyaloshinskii-Moriya (“chiral biquadratic”) interaction that generates weak ferromagnetism *and* couples the ferro- and the altermagnetic order parameters; finally, weak ferromagnetism couples to external magnetic field and allow for controlled manipulations of altermagnetic domains. The fact that MnTe really exists and experimentally demonstrates all these features is strongly encouraging and suggest a new road towards altermagnetic spintronics.

VI. METHODS

All calculations presented here used Vienna ab initio Simulation Package (VASP) [22, 23] within projector augmented wave (PAW) method. [31, 32] The Perdew-Burke-Enzerhof (PBE) [33] generalized gradient approximation was employed to describe exchange-correlation effects. To improve the description for localized d-electrons in Mn^{2+} ion to be strongly correlated, we added a Hubbard U correction with the fully localized limit double-counting recipe [34, 35], with the effective parameter $U - J = 4$ eV. Pseudopotential from the VASP library, PAW_PBE-Te and PAW_PBE-Mn.pv were used, with the energy cutoff of 500 eV, and $9 \times 9 \times 7$ (160 irreducible k-points) mesh.

Some of the figures were generated using VESTA software [36].

ACKNOWLEDGMENTS

This work was supported by the Army Research Office under Cooperative Agreement Number W911NF-22-2-0173. The author is thankful to Nirmal Ghimire, Libor Šmejkal, Jairo Sinova, Stefan Blügel and especially Kirill Belashchenko for valuable discussions.

-
- [1] L. Šmejkal, J. Sinova, and T. Jungwirth, Beyond conventional ferromagnetism and antiferromagnetism: A phase with nonrelativistic spin and crystal rotation symmetry, *Phys. Rev. X* **12**, 031042 (2022).
- [2] L. Šmejkal, J. Sinova, and T. Jungwirth, Emerging research landscape of altermagnetism, *Phys. Rev. X* **12**, 040501 (2022).

- [3] I. Mazin (The PRX Editors), Editorial: Altermagnetism—a new punch line of fundamental magnetism, *Phys. Rev. X* **12**, 040002 (2022).
- [4] T. Berlijn, P. C. Snijders, O. Delaire, T. A. Zhou, H. D. and Maier, and H. B. Cao, Itinerant antiferromagnetism in RuO_2 , *Physical review letters* **118**, 077201 (2017).

- [5] M. Hiraishi, H. Okabe, A. Koda, R. Kadono, T. Muroi, D. Hirai, and Z. Hiroi, Nonmagnetic ground state in RuO₂ revealed by muon spin rotation, *Phys. Rev. Lett.* **132**, 166702 (2024).
- [6] P. Keßler, L. Garcia-Gassull, A. Suter, T. Prokscha, Z. Salman, D. Khalyavin, P. Manuel, F. Orlandi, I. I. Mazin, R. Valentí, and S. Moser, Absence of magnetic order in RuO₂: insights from μ SR spectroscopy and neutron diffraction (2024), arXiv:2405.10820 [cond-mat.mtrl-sci].
- [7] S. G. Jeong, I. H. Choi, S. Nair, L. Buiarelli, B. Pourbahari, J. Y. Oh, N. Bassim, A. Seo, W. S. Choi, R. M. Fernandes, T. Birol, L. Zhao, J. S. Lee, and B. Jalan, Altermagnetic polar metallic phase in ultra-thin epitaxially-strained RuO₂ films (2024), arXiv:2405.05838.
- [8] P. J. Brown, J. B. Forsyth, V. Nunez, and F. Tasset, The low-temperature antiferromagnetic structure of mn5si3 revised in the light of neutron polarimetry, *Journal of Physics: Condensed Matter* **4**, 10025 (1992).
- [9] P. J. Brown and J. B. Forsyth, Antiferromagnetism in mn5si3: the magnetic structure of the af2 phase at 70 k, *Journal of Physics: Condensed Matter* **7**, 7619 (1995).
- [10] M. Gottschilch, O. Gourdon, J. Persson, C. de la Cruz, V. Petricek, and T. Brueckel, Study of the antiferromagnetism of Mn₅Si₃: an inverse magnetocaloric effect material, *J. Mater. Chem.* **22**, 15275 (2012).
- [11] A. Basit, J. Xin, Y. Luo, J.-Y. Y. Dai, and J. Yang, Enhanced thermoelectric performance of MnTe by decoupling of electrical and thermal transports, *Advanced Electronic Materials* **10**, 2300809 (2024).
- [12] J. Wasscher, Evidence of weak ferromagnetism in MnTe from galvanomagnetic measurements, *Solid State Communications* **3**, 169 (1965).
- [13] M. Angadi and V. Thanigaimani, Hall effect in mnte films, *Thin Solid Films* **237**, 187 (1994).
- [14] I. I. Mazin, Altermagnetism in MnTe: Origin, predicted manifestations, and routes to detwinning, *Phys. Rev. B* **107**, L100418 (2023).
- [15] R. D. Gonzalez Betancourt, J. Zubáč, R. Gonzalez-Hernandez, K. Geishendorf, Z. Šobáň, G. Springholz, K. Olejník, L. Šmejkal, J. Sinova, T. Jungwirth, S. T. B. Goennenwein, A. Thomas, H. Reichlová, J. Železný, and D. Kriegner, Spontaneous anomalous hall effect arising from an unconventional compensated magnetic phase in a semiconductor, *Phys. Rev. Lett.* **130**, 036702 (2023).
- [16] K. P. Kluczyk, K. Gas, M. J. Grzybowski, P. Skupinski, M. A. Borysiewicz, T. Fas, J. Suffczynski, J. Z. Domagala, K. Graszka, A. Mycielski, M. Baj, K. H. Ahn, K. Výborný, M. Sawicki, and M. Gryglas-Borysiewicz, Coexistence of anomalous hall effect and weak net magnetization in collinear antiferromagnet MnTe (2023), arXiv:2310.09134.
- [17] M. Chilcote, A. R. Mazza, Q. Lu, I. Gray, Q. Tian, Q. Deng, D. Moseley, A.-H. Chen, J. Lapano, J. S. Gardner, G. Eres, T. Z. Ward, E. Feng, H. Cao, V. Lauter, M. A. McGuire, R. Hermann, D. Parker, M.-G. Han, A. Kayani, G. Rimal, L. Wu, T. R. Charlton, R. G. Moore, and M. Brahlek, Stoichiometry-induced ferromagnetism in altermagnetic candidate MnTe, *Advanced Functional Materials* , 2405829 (2024).
- [18] N. G. Ghimire and et al, to be published.
- [19] D. Kriegner, H. Reichlova, J. Grenzer, W. Schmidt, E. Ressouche, J. Godinho, T. Wagner, S. Y. Martin, A. B. Shick, V. V. Volobuev, G. Springholz, V. Holý, J. Wunderlich, T. Jungwirth, and K. Výborný, Magnetic anisotropy in antiferromagnetic hexagonal MnTe, *Phys. Rev. B* **96**, 214418 (2017).
- [20] E. Turov, Conditions for the existence of weak ferromagnetism and the classification of weakly ferromagnetic structures, *Soviet Phys. JETP* **15**, 1098 (1962).
- [21] W. Kim, I. J. Park, H. J. Kim, W. Lee, S. J. Kim, and C. S. Kim, Room-temperature ferromagnetic property in mnte semiconductor thin film grown by molecular beam epitaxy, *IEEE Transactions on Magnetics* **45**, 2424 (2009).
- [22] G. Kresse and J. Hafner, Ab initio molecular dynamics for liquid metals, *Phys. Rev. B* **47**, 558 (1993).
- [23] G. Kresse and J. Furthmüller, Efficient iterative schemes for ab initio total-energy calculations using a plane-wave basis set, *Phys. Rev. B* **54**, 11169 (1996).
- [24] H. Katsumoto, Y. Mokrousov, and S. Blügel, to be published.
- [25] S. Brinker, M. dos Santos Dias, and S. Lounis, The chiral biquadratic pair interaction, *New Journal of Physics* **21**, 083015 (2019).
- [26] A. Lászlóffy, L. Rózsa, K. Palotás, L. Udvardi, and L. Szunyogh, Magnetic structure of monatomic Fe chains on re(0001): Emergence of chiral multispin interactions, *Phys. Rev. B* **99**, 184430 (2019).
- [27] T. Moriya, Theory of magnetism of NiF₂, *Phys. Rev.* **117**, 635 (1960).
- [28] C. Zener, Interaction between the *d*-shells in the transition metals. ii. ferromagnetic compounds of manganese with perovskite structure, *Phys. Rev.* **82**, 403 (1951).
- [29] D. I. Khomskii, *Basic aspects of the quantum theory of solids* (Cambridge University Press, 2010).
- [30] J. K. Glasbrenner, I. Žutić, and I. I. Mazin, Theory of Mn-doped II-II-V semiconductors, *Phys. Rev. B* **90**, 140403 (2014).
- [31] P. E. Blöchl, Projector augmented-wave method, *Phys. Rev. B* **50**, 17953 (1994).
- [32] G. Kresse and D. Joubert, From ultrasoft pseudopotentials to the projector augmented-wave method, *Phys. Rev. B* **59**, 1758 (1999).
- [33] J. P. Perdew, K. Burke, and M. Ernzerhof, Generalized gradient approximation made simple, *Phys. Rev. Lett.* **77**, 3865 (1996).
- [34] A. I. Liechtenstein, V. I. Anisimov, and J. Zaanen, Density-functional theory and strong interactions: Orbital ordering in Mott-Hubbard insulators, *Phys. Rev. B* **52**, R5467 (1995), publisher: American Physical Society.
- [35] S. L. Dudarev, G. A. Botton, S. Y. Savrasov, C. J. Humphreys, and A. P. Sutton, Electron-energy-loss spectra and the structural stability of nickel oxide: An LSDA+U study, *Phys. Rev. B* **57**, 1505 (1998), publisher: American Physical Society.
- [36] K. Momma and F. Izumi, VESTA 3 for three-dimensional visualization of crystal, volumetric and morphology data (2011).